Received: 20 October 2020 | Revised: 18 January 2021 | Accepted: 10 February 2021

DOI: 10.1002/mrd.23461

Molecular Reproduction & Development

RESEARCH ARTICLE

Sperm chromatin integrity and DNA methylation in Norwegian Red bulls of contrasting fertility

Birgitte Narud[1,2] | Abdolrahman Khezri[2] | Teklu Tewoldebrhan Zeremichael[2] | Else-Berit Stenseth[2] | Bjørg Heringstad[3] | Anders Johannisson[4] | Jane M. Morrell[4] | Philippe Collas[1,5] | Frøydis Deinboll Myromslien[2] | Elisabeth Kommisrud[2]

[1]Department of Molecular Medicine, Institute of Basic Medical Sciences, University of Oslo, Oslo, Norway

[2]Department of Biotechnology, Inland Norway University of Applied Sciences, Hamar, Norway

[3]Department of Animal and Aquacultural Sciences, Faculty of Biosciences, Norwegian University of Life Sciences, Ås, Norway

[4]Department of Clinical Sciences, Swedish University of Agricultural Sciences, Uppsala, Sweden

[5]Department of Immunology and Transfusion Medicine, Oslo University Hospital, Oslo, Norway

Correspondence

Elisabeth Kommisrud, Department of Biotechnology, Inland Norway University of Applied Sciences, P.O. Box 400, 2418 Elverum, Norway.
Email: elisabeth.kommisrud@inn.no

Funding information

The Research Council of Norway

Abstract

In this study, the complexity of chromatin integrity was investigated in frozen-thawed semen samples from 37 sires with contrasting fertility, expressed as 56-day non-return rates (NR56). Protamine deficiency, thiols, and disulfide bonds were assessed and compared with previously published data for DNA fragmentation index (DFI) and high DNA stainability (HDS). In addition, in vitro embryo development and sperm DNA methylation were assessed using semen samples from 16 of these bulls. The percentages of DFI and HDS were negatively associated with NR56 and cleavage rate and positively associated with sperm protamine deficiency ($p < 0.05$). Significant differences in cleavage and blastocyst rates were observed between bulls of high and low NR56. However, once fertilization occurred, further development into blastocysts was not associated with NR56. The differential methylation analysis showed that spermatozoa from bulls of low NR56 were hypermethylated compared to bulls of high NR56. Pathway analysis showed that genes annotated to differentially methylated cytosines could participate in different biological pathways and have important biological roles related to bull fertility. In conclusion, sperm cells from Norwegian Red bulls of inferior fertility have less compact chromatin structure, higher levels of DNA damage, and are hypermethylated compared with bulls of superior fertility.

KEYWORDS

bull sperm, chromatin integrity, in vitro fertilization, non-return rate, sperm DNA methylation

1 | INTRODUCTION

The main task of the sperm cell is to deliver the paternal genome to an oocyte during fertilization. Sperm DNA integrity is crucial for successful fertilization and subsequent embryo development (Kumaresan et al., 2020). The sperm cell has a unique chromatin structure where most of the histones are replaced by smaller proteins, called protamines, during spermatogenesis (Champroux et al., 2018). This histone to protamine transition facilitates tight packaging of DNA in the sperm nucleus. However, sperm DNA is still susceptible to damage (McSwiggin & O'Doherty, 2018). A wide range of intrinsic and extrinsic factors may cause sperm DNA fragmentation,

including oxidative stress, abortive apoptosis, deficiencies in recombination, age, semen handling, thermal stress, vaccinations, and bacterial infections (González-Marín et al., 2012; Kumaresan et al., 2020). Studies have shown that the degree of sperm DNA fragmentation is negatively correlated with bovine field fertility (Gliozzi et al., 2017; Narud et al., 2020; Waterhouse et al., 2006) and the outcome of in vitro fertilization (IVF) (Fatehi et al., 2006; Simões et al., 2013). Further, the histone to protamine ratio in sperm cells affects male fertility, where infertile men possess sperm cells with higher proportions of retained histones compared to fertile men (X. Zhang et al., 2006). Protamine deficiency may be considered as a contributing factor to DNA instability and damage (Boe-Hansen et al., 2018). The highly compacted structure of sperm chromatin is dependent on the number of disulfide bonds within and between protamines (Oliva, 2006). Assessment of free thiols and disulfide bonds in combination with protamine deficiency analysis may provide useful information regarding sperm chromatin compaction (Martínez-Pastor et al., 2010). However, there are disagreements between studies whether or not the degree of protamination of bull spermatozoa are associated with sperm chromatin integrity (Castro et al., 2018; Fortes et al., 2014). Fertilization of an oocyte by a sperm cell with damaged DNA may affect embryo development negatively and contribute to diseases in future generations, as the oocyte only has the ability to correct a certain degree of DNA damage (Johnson et al., 2011; Ménézo et al., 2010). Sperm cells deliver epigenetic components to the oocyte, essential to successful fertilization and embryonic development (Kropp et al., 2017). The term epigenetics refers to the study of heritable changes in gene expression that occur without altering the DNA sequence (McSwiggin & O'Doherty, 2018). The most thoroughly studied epigenetic modification is DNA methylation, which has emerged as a promising indicator of male infertility (Kumaresan et al., 2020). The mechanism behind DNA methylation is an addition of a methyl group to the 5th carbon of a cytosine immediately followed by a guanine (CpG dinucleotide) (Alkhaled et al., 2018; Urrego et al., 2014). Sperm DNA methylation signatures have been associated with the fertility status of bulls (Kropp et al., 2017), buffalo (Verma et al., 2014), and men (Alkhaled et al., 2018). Studies on DNA methylation in bull spermatozoa are, however, still limited. Increased knowledge within the field would benefit livestock breeding by providing information regarding possible heritable traits and predisposition of diseases (Triantaphyllopoulos et al., 2016). Reduced representation bisulphite sequencing (RRBS) is a high-throughput and cost-efficient DNA methylation analysis method, allowing the study of DNA methylation at a single-base resolution (Doherty & Couldrey, 2014; Meissner et al., 2005). Analysis of DNA methylation using RRBS has previously been conducted for bovine somatic tissues and spermatozoa (Khezri et al., 2020; Perrier et al., 2018; Zhou et al., 2016).

Recently, we showed that the chromatin integrity parameters DNA fragmentation index (DFI) and high DNA stainability (HDS) in sperm cells from Norwegian Red bulls were significantly negatively associated with field fertility, expressed as 56-day non-return rate (NR56) (Narud et al., 2020). The aim of the present study was to evaluate several parameters related to sperm chromatin integrity in Norwegian Red bulls of contrasting NR56. The analyses included evaluation of protamine deficiency, free thiols, and disulfide bonds. In addition, in vitro embryo development and sperm DNA methylation signatures were assessed.

2 | MATERIAL AND METHODS

2.1 | Animals and semen processing

Cryopreserved semen samples were provided by the breeding company Geno (Geno Breeding and Artificial Insemination (AI) Association). Bulls were raised and fed uniformly and cared for according to the Norwegian Animal Welfare Act (LOV 2009-06-19 no. 97). The semen production procedures were in compliance with European Union Directive 88/407.

Sires were selected based on their field fertility performance, measured as NR56, as previously described by Narud et al. (2020). In brief, data on AIs were collected from the Norwegian Dairy Herd Recording System (NDHRS). The General Linear Model (PROC GLM in SAS®) was used to calculate least square mean (LSmean) NR56 for 507 Norwegian Red bulls used for AI in the period 2013-2018. The model included effects of bull, month and year of AI, parity of the female and repeated AI within 1–4 days. Based on these results, a group of 19 bulls with high NR56 (hereafter referred to as HF) and a group of 18 bulls with low NR56 (hereafter referred to as LF) were selected. LSmean NR56 ranged from 0.76 to 0.78 for HF and from 0.46 to 0.65 for LF (Table 1). All bulls were in regular semen production, with a mean (±*SD*) age corresponding to the collection date of ejaculates analyzed in vitro being 517 (±162) days for HF and 459 (±35) days for LF bulls. The age of the bulls in the two groups was not different ($p > 0.05$). For the in vitro production (IVP) of embryos and the analysis of sperm DNA methylation by RRBS, eight bulls with high and low NR56 were selected (marked by asterisk in Table 1). Pedigree information was considered to avoid including closely related individuals.

Post collection, ejaculates with motility above 70% and morphological abnormalities below 15% were diluted to a final concentration of 12×10^6 spermatozoa per AI dose in French mini straws (IMV). A two-step dilution procedure with Biladyl® extender containing glycerol (Minitube, 13500/0004-0006) and fresh egg yolk was applied. Cryopreservation was performed according to standard procedures (Standerholen et al., 2014) and the semen doses were stored in liquid nitrogen (−196°C) until use.

2.2 | Preparation of samples for protamine deficiency and thiol assays

Two semen straws per bull were thawed at 37°C for 12 s and mixed. For four of the bulls, only one straw was available. The concentration of spermatozoa was determined with a Nucleocounter SP-100

TABLE 1 Field fertility (LSmean NR56), age (days) at semen collection for in vitro analyses and number of inseminations for the bulls used in the study

Low NR56				High NR56			
Bull	Age	NR56	No. AIs.	Bull	Age	NR56	No. AIs.
LF1*	481	0.46	689	HF1	447	0.76	831
LF2*	439	0.53	803	HF2	478	0.76	821
LF3	542	0.55	805	HF3	474	0.76	842
LF4*	443	0.58	695	HF4	449	0.76	651
LF5*	500	0.61	713	HF5	1083	0.76	8542
LF6	413	0.62	840	HF6	428	0.76	686
LF7	432	0.63	837	HF7	458	0.76	922
LF8	460	0.63	976	HF8	449	0.76	986
LF9*	510	0.63	791	HF9	467	0.76	857
LF10*	454	0.64	922	HF10	787	0.76	4156
LF11	489	0.64	318	HF11*	422	0.76	611
LF12*	421	0.64	652	HF12*	422	0.76	825
LF13	453	0.64	333	HF13*	423	0.77	764
LF14	487	0.65	204	HF14*	553	0.77	710
LF15*	414	0.65	751	HF15*	571	0.77	1069
LF16	434	0.65	708	HF16*	419	0.77	2149
LF17	440	0.65	700	HF17*	453	0.78	767
LF18	457	0.65	899	HF18	485	0.78	496
				HF19*	556	0.78	2555

Note: Asterisks mark the 16 bulls used for in vitro fertilization and sperm DNA methylation analysis.

(ChemoMetec). Further, each sample was split in two, one part of the sample was diluted in 400 µl TNE-buffer (0.01 mol/L of Tris-HCl, 0.15 mol/L of NaCl, and 1 mmol/L of EDTA, pH 7.4) and used for analysis of protamine deficiency, while the other was diluted in 1100 µL TNE-buffer and used for analysis of thiols and disulfide bonds. In both sample preparations, the final concentration was 2×10^6 cells/ml. Quadruplicates of both sample types were then snap-frozen in liquid nitrogen.

2.3 | Analysis of protamine deficiency

The level of sperm protamine deficiency was assessed using chromomycin A_3 (CMA3; Sigma-Aldrich), as described by Zubkova et al. (2005) with minor modifications. Briefly, snap-frozen samples were thawed on ice and washed with phosphate-buffered saline (PBS) by centrifugation (300 x *g* for 10 min). The resulting sperm pellet was resuspended in 80 µl McIlvaine's buffer (17 ml 0.1 mol/L citric acid mixed with 83 ml 0.2 mol/L Na_2HPO_4 and 10 mmol/L $MgCl_2$, pH 7.0) containing 0.25 mg/ml CMA3. Further, the samples were incubated in the dark for 20 min at 37°C and washed in 400 µl PBS by centrifugation (300 x *g* for 10 min). Pellets were resuspended in 400 µl PBS containing 3.2 µl propidium iodide (PI, 2.4 mM solution; Molecular Probes). A flow cytometer (FACSVerse; BD Biosciences) equipped with a blue laser (488 nm) was utilized for analysis of the samples. Gating of the sperm cell population was performed using forward scatter (FSC) and side scatter (SSC) and sperm cells were further identified by PI positive signal collected via 586/42 bandpass filter. After excitation with a violet laser (405 nm), the CMA3 fluorescence from gated cells was collected through a 528/45 bandpass filter.

2.4 | Analysis of thiols and disulfide bonds

Free thiols, total thiols, and disulfide bonds in bull spermatozoa were analyzed using monobromobimane (mBBr; Molecular Probes), according to the previously described method by Zubkova et al. (2005) and Seligman et al. (1994) with some modifications. Briefly, the samples were thawed on ice and divided into two tubes, each containing 1×10^6 sperm cells. The first tube was incubated with 1 mmol/L of 1,4-dithiothreitol (DTT; Sigma-Aldrich) for 10 min at 37°C, while no DTT was added to the second tube. After centrifugation of both tubes (300 x *g* for 10 min), the pellets were resuspended in 100 µl PBS containing 0.5 mmol of mBBr solution. Both tubes were incubated in the dark for 10 min at 37°C, washed with 500 µl PBS twice by centrifugation (300 x *g* for 10 min). The pellets were resuspended in 500 µl PBS and analyzed with a FACSVerse flow cytometer (BD Biosciences) after excitation of mBBr by a 405 nm violet laser. The mBBr fluorescence was collected by a 528/45 bandpass filter, and gating of the sperm cell population was done using FSC and SSC. To calculate disulfide concentrations, the fluorescence signals of free thiols (mBBr fluorescence from non-DTT-treated sample) were subtracted from fluorescence signals of total thiols (mBBr fluorescence from DTT-treated sample), thereafter that value was divided by two. After the initial run, 4 µl PI (2.4 mM solution; Molecular Probes) was added to each sample, and the samples were analyzed again, this time also collecting the PI-fluorescence through a 586/42 bandpass filter. These data were used only as a further aid to discriminate debris from spermatozoa and were not used for quantitative purposes, since the PI was found to quench the mBBr-fluorescence.

2.5 | IVP of bovine embryos

IVP of embryos was conducted using media from IVF biosciences (Falmouth). Eight bulls with low NR56 and eight bulls with high NR56 were used for IVF. For each experiment, oocytes were randomly split into groups of 30 oocytes and two groups were fertilized with frozen-thawed semen from the same bull. Two LF and two HF bulls were used for fertilization in each test week. In addition, a reference bull with known IVF performance was used as control throughout the study. Each IVF experiment was repeated three times and a total of 180 oocytes per bull were included.

2.5.1 | Oocyte collection and in vitro maturation

Bovine ovaries were collected at a local slaughterhouse and transported in warm (30°C to 33°C) saline solution (0.9% NaCl, 2.5 ml 1% kanamycin) to the laboratory within 4 h. Cumulus–oocyte complexes (COCs) were aspirated from follicles sized 3–15 mm in diameter and collected in a 50 ml falcon tube containing 140 µl heparin (5.000 IU/ml). After settling at the bottom of the tube, the oocyte pellet was transferred to a dish containing Wash-medium (Falmouth). The COCs were thereafter washed three times by transferring them to new dishes of Wash-medium. Groups of good quality COCs (grade I and II according to Blondin and Sirard (1995)) were selected and finally transferred in groups of 30 to 4-well plates (NuncTM, 734-2693; Thermo Fisher Scientific, VWR Norway) containing 500 µl of BO-IVM media (Falmouth). The COCs were matured for 22–24 h at 38.8°C under an atmosphere of 6% CO_2 in air with maximum humidity.

2.5.2 | IVF and culture

After maturation, the COCs were washed and transferred to new four-well plates containing 500 µl BO-IVF media (Falmouth), and kept in the incubator (38.8°C, 6% CO_2, maximum humidity) while the semen samples were prepared. Two semen straws per bull were thawed in a water bath at 37°C for 1 min and the semen was transferred to the bottom of a 15 ml falcon tube containing preheated (36°C) BO-SemenPrep (Falmouth). The semen samples were centrifuged (330 x *g* for 5 min), the supernatant was removed, and 4 ml of BO-SemenPrep was added to the pellet. The centrifugation step was repeated, followed by removal of the supernatant, and computer-assisted sperm analysis (CASA) was used for assessing sperm motility and concentration. Sperm was added to each group of oocytes with a final concentration of 1×10^6 progressive motile spermatozoa/ml, followed by 18 h incubation (6% CO_2, 38.8°C, maximum humidity). The presumptive fertilized oocytes were denuded by vortexing, before they were washed and transferred to culture plates containing 500 µl BO-IVC media (Falmouth) with oil overlay. Culture was performed in a humidified atmosphere of 7% O_2, 6% CO_2, and 87% N_2 at 38.8°C. At day 3 post-fertilization, the cleavage rate was recorded. Further, at day 8 the blastocyst rate was calculated based on the total number of oocytes. The number of cleaved cells that developed further into blastocysts was also recorded.

2.6 | RRBS library preparation and Illumina sequencing

Semen samples from eight bulls with low NR56 and eight bulls with high NR56 were utilized for the construction of RRBS libraries using a gel-free multiplexed technique (Boyle et al., 2012), previously optimized to study sperm DNA methylation in boar (Khezri et al., 2019) and bull (Khezri et al., 2020). The protocol consisted of the following steps.

An amount of 100 ηg genomic DNA was digested overnight at 37°C using *MspI* and *Taqα1* enzymes (New England Biolabs). Fragmented DNA was subjected to Gap filling and A-tailing by adding 1 µl of Klenow fragment (New England Biolabs) and 1 µl of dNTP mixture containing 10 mM dATP, 1 mM dCTP, and 1 mM dGTP (New England Biolabs). The processed DNA was further incubated for 20 min at 30°C followed by 20 min at 37°C. Size selection (300–500 bp) was performed by adding a 2× SPRI AMPure XP beads for 30 min at room temperature (RT) (Beckman Coulter). Then samples were placed on a side magnet, the supernatant was removed, and beads were washed and re-suspended in 20 µl elution buffer (Qiagen). Size selected DNA samples were further prepared for Illumina sequencing by ligating the standard Illumina adapters using 2 µl of NEXTflex™ Bisulfite-Seq barcodes (Bio Scientific Corporation) and ligase mixture, followed by incubation overnight at 16°C. Adapter ligated DNA samples were again subjected to size selection by adding 1.5× of 20% PEG 8000/2.5 M NaCl (Amresco Inc.) followed by 30 min incubation at RT. The supernatant was discarded as described previously and beads were washed twice using 70% EtOH followed by resuspension in 25 µl elution buffer (Qiagen). Size selected DNA fragments were bisulfite converted and the product was cleaned up according to recommendations in the QIAGEN EpiTect kit (Gu et al., 2011). Before amplification of bisulfite-converted DNA fragments, various PCR amplification cycles (10, 13, 16, and 19 cycles) were tested. To evaluate the efficiency of the protocol by observing DNA bands and to determine the appropriate PCR amplification cycle, the PCR product were analyzed on a gradient Criterion precast polyacrylamide TBE gel (4%–20%) (Thermo Fisher Scientific). The PCR product (after 13 amplification cycles), were further cleaned up by adding 1× SPRI AMPure XP beads followed by incubation for 30 min at RT. The supernatant was discarded and the beads were washed with 70% EtOH. After 30 s incubation at RT, EtOH was removed, and beads were allowed to dry for 5 min before resuspension in 25 µl elution buffer. Eluted beads were placed on a side magnet for 5 min before transfer of the supernatant (purified libraries) to a clean tube. The DNA concentration of eluted RRBS libraries were measured using PicoGreen dsDNA absorbance method. The prepared libraries were sent to Norwegian Sequencing Centre where sequencing was performed by Illumina HiSeq 4000 in paired-end (2 × 150 bp) mode.

2.7 | Bioinformatics analyses

2.7.1 | Illumina reads quality assessment and trimming

Quality of paired-end Illumina reads was assessed using fastQC software (v 0.11.8 for Linux). Illumina adapters and low-quality sequences (below 20 bp and Phred score of 30) were trimmed using the Trim-galore software (v 0.4.4 for Linux) (Martin, 2011).

2.7.2 | Mapping the clean reads with reference genome

Bull reference genome (*bosTau9*) was downloaded from the UCSC database (UCSC, 2018) and indexed using bismark_genome_preparation in Bismark (v 0.19.0 for Linux) (Krueger & Andrews, 2011). Mapping was performed using the Bismark tool and bowtie2 aligner (v 2.3.2 for Linux) (Krueger & Andrews, 2011) with the following parameters [-n 0 -l 20 and --score-min (L, 0, −0.4)]. Global CpG methylation level in Bismark was calculated for all covered cytosines (Cs) using the following formula: % of global methylation = 100 × number of methylated Cs/number of methylated Cs + number of unmethylated Cs.

2.7.3 | Differential methylation analysis

Differentially methylated cytosines (DMCs) were identified using reads with CpGs ≥ 5× coverage depth (CpG_{5x}) between control (eight HF bulls) and test (eight LF bulls) groups, using the methylKit package (v 1.6.1) (Akalin et al., 2012) in Rstudio (v 1.1.453 for Linux). Before the analysis, reads containing CpGs with more than 99.9th percentile coverage were excluded. After applying logistic regression analysis with a sliding linear model to correct for multiple comparisons only DMCs with ≥10% methylation difference and q value < 0.05 (filtered DMCs onwards) were considered for downstream analysis. In this study, hypermethylated and hypomethylated Cs are defined as differential methylation over 10% or smaller than −10% in the test group compared to the control group, respectively.

2.7.4 | Annotation of DMCs

BED files containing gene and CpG annotation for the *bosTau9* assembly were downloaded from UCSC table browser (UCSC, 2018). Genomation package (v 1.14.0) in Rstudio was employed to annotate filtered DMCs with nearest transcriptional start site (TSS), gene elements (exons, introns, promoters, intergenic regions), and CpG features (CpG islands, CpG shores, other). In this study, promoters and CpG shores were defined as ±1000 bp and ±2000 bp of the TSS and CpG islands, respectively.

2.7.5 | Pathway analysis

Corresponding GenBank accession IDs to annotated TSSs were submitted to DAVID Bioinformatics resources for functional annotation (Huang da et al., 2009) for Gene Ontology (GO) analysis. Gene enrichment for each identified pathway was calculated using Fisher's exact test and the p value was Benjamini corrected for multiple testing and set to 0.05.

2.8 | Statistical analyses

The statistical analyses of the different in vitro sperm quality traits and IVP experiments were performed using SAS Version 9.4 for Microsoft Windows (SAS Institute). The data were tested for normal distribution by the Shapiro-Wilk test. Parameters that did not show a normal distribution (DFI and HDS) were log-transformed before further statistical analyses. Differences in sperm chromatin integrity parameters between HF and LF bulls were assessed by unpaired t test, including the folded F test for equality of variances. Differences in cleavage and blastocyst rate (calculated as % development from fertilized oocytes and % development from cleaved cells) between LF and HF bulls were studied using mixed linear model (proc mixed). Fertility group (0 [LF] or 1 [HF]), replicate of bull (1, 2, 3) and test week (1, 2, 3, 4) were included in the model as fixed effects, and bull (1 to 16) was included as random effect. Correlation coefficients (Pearson) were calculated and considered statistically significant when $p < .05$.

The RRBS results were plotted using GraphPad Prism (v 6.01 for Windows, GraphPad Software). The Venny online platform (Oliveros, 2015) and ggplot2 package (v 3.1.0) in Rstudio (Wickham, 2016) were employed to construct Venn diagrams and plot pathway analysis results, respectively.

3 | RESULTS

3.1 | Sperm chromatin integrity analyses

Sperm quality parameters related to chromatin integrity for the two fertility groups are presented in Table 2. As previously reported in Narud et al. (2020), higher percentages of DFI ($p < 0.001$) and HDS ($p < 0.01$) were observed in sperm cells from LF bulls compared to HF bulls. The mean levels of free thiols, total thiols, disulfide bonds, and protamine deficiency were not different ($p > 0.05$) for LF bulls compared with HF bulls.

The chromatin integrity parameters were further subjected to Pearson correlation analysis to identify possible relationships with NR56 and among parameters. As presented in Narud et al. (2020), DFI and HDS correlated negatively with NR56. Furthermore, the results presented in Table 3 shows that DFI and HDS correlated positively with each other and with protamine deficiency. The number of disulfide bonds was strongly (positively) correlated with total thiols.

3.2 | IVF and embryo development

A higher proportion of oocytes cleaved after fertilization with sperm from bulls of high (71.3% ± 10.6) compared to low (53.8% ± 13.7) NR56 ($p < 0.05$) (Figure 1). Further, there was a higher proportion of blastocysts at day 8 for the HF bulls (27.9% ± 6.1) than for the LF bulls (20.5% ± 6.3) ($p < 0.05$). The proportion of cleaved cells that developed further into day 8 blastocysts was not different between the two fertility groups (HF: 39.1% ± 6.3, LF: 38.0% ± 4.8) ($p > 0.05$).

TABLE 2 Sperm quality parameters related to chromatin integrity in semen samples from bulls of low ($n = 18$) and high ($n = 19$) NR56

	Low NR56	High NR56
DFI (%)[a]		
Min–max	1.67–6.5	1.0–4.0
Mean ± *SD*	3.5 ± 1.4	1.8 ± 0.8**
HDS (%)[a]		
Min–max	1.5–7.2	1.6–5.1
Mean ± *SD*	4.3 ± 1.7	2.9 ± 1.2*
Free thiols (mFI)		
Min–max	3609.0–11,303.0	6470.0–10,849.0
Mean ± *SD*	8184.0 ± 2144.0	8464.1 ± 1233.7
Total thiols (mFI)		
Min–max	32,115.0–47,524.0	30,121.0–47,372.0
Mean ± *SD*	40,593.3 ± 5023.8	41,659.4 ± 4087.2
Disulfide bonds (mFI)		
Min–max	11,721.0–20,190.0	11,482.0–19,722.0
Mean ± *SD*	16,204.7 ± 2378.6	16,597.6 ± 2018.4
Protamine deficiency (mFI)		
Min–max	2429.0–4305.0	2347.0–3475.0
Mean ± *SD*	3134.5 ± 455.1	2890.7 ± 347.3

Note: Results are presented as range (min–max) and mean ± *SD*. For protamine deficiency, $n = 15$ and $n = 18$ for bulls of low and high NR56, respectively. Asterisks indicate significant differences between the groups: *$p < 0.01$, **$p < 0.0001$.

Abbreviations: DFI, DNA fragmentation index; HDS, high DNA stainable; mFI, mean fluorescence intensity; NR56, 56-day non-return rate.

[a]Data from Narud et al. (2020).

3.3 | Correlations between NR56, chromatin integrity traits and in vitro embryo development

Pearson correlation analysis indicated a positive relationship between NR56 and in vitro embryo development (Table 4). The cleavage rate was negatively correlated with DFI and HDS ($p < 0.05$). There were no correlations ($p > 0.05$) between the proportion of cleaved cells that further developed into day 8 blastocysts and any of the chromatin integrity parameters.

3.4 | Basic statistics of RRBS libraries

An overview of the basic statistics for the RRBS libraries is presented in Table 5. After removing low-quality reads and Illumina adapters, 94% of reads were saved. The RRBS libraries had an average of 14.6 million reads per sample and 30.5× read coverage compared to in silico created RRBS genome. Trimmed reads had on average 99% conversion rate and mapping against reference genome resulted in 34.7% unique mapping efficiency. Furthermore, on average, 741,000 CpG_{5x}, with methylation average of 42.8% were covered in RRBS libraries. None of the parameters for mapping efficiency, global CpG methylation level and conversion rate were significantly different ($p > 0.05$) between LF bulls compared with HF bulls. The correlation between global CpG level and embryo development was also assessed; however, no correlations were detected ($p > 0.05$).

Cluster analysis according to CpG_{5x} methylation value showed that the samples were not clustered based on fertility performance (Figure 2). Furthermore, Pearson's correlation coefficient based on the same criteria revealed a high positive correlation between samples regarding CpG_{5x} methylation profile (Pearson's correlation coefficient > 0.94) (Table S1).

3.5 | Differential methylation analysis

By applying a significance cut-off equal to q value < 0.05, a total number of 16,542 DMCs were detected with varying degree of methylation, ranging from 0% to 75%. Majority of DMCs (56%) were found to be hypermethylated in the LF group compared to the HF group (Figure 3a). After applying a 10% methylation cut-off, 65% of DMCs had over 10% methylation difference in both hypo- and hypermethylated groups (Figure 3b). Applying a 10% methylation cut-off resulted in 10,772 DMCs (filtered DMCs), which were further used for downstream analyses (Figure 3c).

3.6 | Annotation of DMCs with gene and CpG features

Annotation of filtered DMCs in both hypomethylation and hypermethylation groups with gene features revealed similar trends.

TABLE 3 Pearson's correlation coefficients and p values (in brackets) between sperm chromatin integrity traits and NR56 ($n = 37$, except for PD where $n = 33$)

	NR56	DFI[a]	HDS[a]	FT	TT	DB
DFI[a]	−0.57 (<0.0001)*					
HDS[a]	−0.37 (0.03)*	0.63 (<0.0001)*				
FT	−0.01 (0.97)	−0.09 (0.59)	0.07 (0.68)			
TT	0.13 (0.43)	−0.13 (0.43)	−0.19 (0.27)	0.29 (0.08)		
DB	0.14 (0.40)	−0.10 (0.55)	−0.22 (0.19)	−0.09 (0.59)	0.93 (<0.0001)*	
PD	−0.23 (0.20)	0.40 (0.02)*	0.45 (0.01)*	0.21 (0.23)	0.07 (0.71)	−0.01 (0.96)

Note: Asterisks indicate significant correlations ($p < 0.05$).

Abbreviations: DB, disulfide bonds; DFI, DNA fragmentation index; FT, free thiols; HDS, high DNA stainable; NR56, 56-day non-return rate; PD, protamine deficiency; TT, total thiols.

[a]Data from Narud et al. (2020).

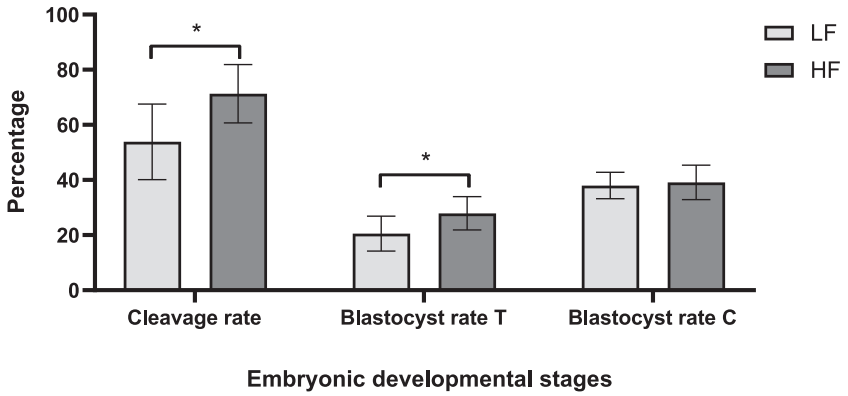

FIGURE 1 Mean cleavage and blastocyst rates (*SD* given as whiskers) following in vitro fertilization of oocytes with sperm from bulls with high (HF) and low (LF) 56 days non-return rate ($n = 8$ in each group). Asterisks indicate a significant difference between the two fertility groups ($p < 0.05$) based on a linear mixed model. The blastocyst rate was assessed on day 8 and is expressed as Blastocyst rate T: % blastocysts developed from total number of oocytes and Blastocyst rate C: % blastocysts developed from the cleaved oocytes

For instance, 70% of the filtered DMCs were present in the intergenic regions followed by introns, exons, and promoters (Figure 4a). Furthermore, over 85% of filtered DMCs in both hypomethylation and hypermethylation groups were annotated within regions outside of CpG islands (CGI)/CGI shores. Only around 15% of filtered DMCs were annotated within CGI/CpG shores (Figure 4b).

3.7 | Pathway analysis

Before pathway analysis, DMCs ≥ 10% were annotated with the nearest transcription start sites (TSSs) (Figure 5a). Annotation results showed a greater number of TSSs in the hypermethylation group (3274 TSSs) compared with the hypomethylation group (2727 TSSs). A total number of 1287 TSSs were harbored with both hypomethylated and hypermethylated Cs. Pathway analyses showed that TSSs in hyper- and hypomethylated groups, contributed to a total number of 50 and 23 significant pathways, respectively. Among those, 18 pathways were detected as mutual pathways associated with TSSs harbored with both hypo- and hypermethylated Cs (Figure 5b).

We were particularly interested in genes associated with biological processes related to fertility. Table 6 shows that the number of such identified genes were higher in the hypermethylation group compared with the hypomethylation group. Genes related to the penetration of zona pellucida was identified exclusively in the hypermethylation group. In both hypo- and hypermethylation groups biological processes including in utero embryo development, followed by fertilization and embryo implantation, were represented by the highest numbers of genes (Table S2).

Pathway analysis showed that the majority of identified mutual pathways between hypomethylated and hypermethylated groups exhibited similar *p* values (Figure S1). Moreover, the majority of exclusively identified pathways (32 pathways) were in association with genes close to hypermethylated cytosines. Only five pathways were linked to genes close to hypomethylated cytosines (Figure 6). Several pathways were exclusively identified in the hypermethylation group of test samples (LF bulls). This included hormonal pathways such as oxytocin signaling and ion-related signaling pathways such as calcium signaling, ion channel/transport, and voltage-gated channel, which all play a direct role in the fertilization process. Furthermore, pathways involved in embryonic development such as developmental proteins and vascular endothelial growth factor (VEGF) signaling pathway were exclusively identified in the hypermethylation group of LF bulls.

TABLE 4 Pearson correlation coefficients (corr.) between NR56, the chromatin integrity parameters, and cleavage rate and total blastocyst rate ($n = 16$)

	Cleavage rate		Blastocyst rate T	
	Corr.	*p* value	Corr.	*p* value
NR56	0.56	0.025*	0.50	0.051*
DFI (%)	−0.56	0.025*	−0.45	0.084
HDS (%)	−0.50	0.048*	−0.29	0.274
FT (mFI)	0.43	0.100	0.34	0.204
TT (mFI)	0.22	0.408	0.40	0.127
DB (mFI)	0.01	0.969	0.23	0.388
PD (mFI)	−0.08	0.789	0.17	0.587

Note: Asterisks indicate correlations significantly different from 0 ($p \leq 0.05$).

Abbreviations: Blastocyst rate T, % blastocysts developed from the total number of oocytes; DB, disulfide bonds; DFI, DNA fragmentation index; HDS, high DNA stainable; FT, free thiols; mFI, mean fluorescence intensity; NR56, 56-day non-return rate; PD, protamine deficiency; TT, total thiols.

4 | DISCUSSION

In the current study, various chromatin integrity parameters in semen samples from 37 Norwegian Red bulls of low and high NR56 were analyzed. Furthermore, 16 of these bulls were selected for IVP

TABLE 5 Summary statistics for reduced representation bisulphite sequencing libraries

Bull ID	Total reads	Clean reads after trimming (percentage of retrieved reads)	Read coverage (X)	Unique mapping efficiency (%)	Global CpG methylation (%)	Number of 5x CpGs	Bisulphite conversion rate (%)
HF 1	13,657,477	12,754,713 (93.4)	26.5	36.9	43.3	660,513	99.1
HF 2	14,127,957	13,309,272 (94.2)	28.0	35.6	42.6	657,272	99.0
HF 3	15,231,439	14,336,622 (94.1)	30.0	33.9	41.9	700,034	99.1
HF 4	17,031,740	15,961,764 (93.7)	34.3	30.2	44.0	645,608	99.0
HF 5	20,397,755	19,240,081 (94.3)	39.9	34.3	42.2	1,361,145	99.0
HF 6	15,623,143	14,728,278 (94.3)	30.8	35.9	43.1	840,029	99.0
HF 7	12,725,025	11,911,015 (93.6)	25.7	36.2	43.2	537,377	99.0
HF 8	11,189,589	10,489,998 (93.7)	22.8	38.6	45.0	533,764	99.0
LF 1	12,484,969	11,708,651 (93.8)	24.7	36.0	42.9	462,950	98.9
LF 2	16,053,221	15,124,114 (94.2)	30.4	33.3	42.6	684,065	99.0
LF 3	15,345,745	14,462,408 (94.2)	29.2	32.4	42.2	573,138	98.8
LF 4	19,046,631	18,537,954 (97.3)	39.5	31.6	39.6	943,073	98.9
LF 5	18,701,716	17,621,093 (94.2)	36.2	30.4	41.1	740,494	99.0
LF 6	16,619,280	15,562,528 (93.6)	32.8	37.3	44.9	937,896	98.9
LF 7	13,472,993	12,679,214 (94.1)	25.8	34.7	42.9	513,328	99.0
LF 8	15,603,965	14,562 799 (93.3)	32.6	38.7	44.1	1,072,109	99.1

Note: Libraries were created from sperm DNA collected from bulls with high (HF) and low (LF) NR56 ($n = 8$ in each group). Clean reads were obtained after adapter and low-quality trimming of Illumina sequencing reads (total reads). Read coverage was calculated by dividing the number of bp in the clean reads by the number of bp at in silico MspI-digested *bosTau9* genome. Mapping efficiency shows the percentage of clean reads that mapped with unique positions at *bosTau9* genome. Global CpG methylation indicate the percentage of methylated CpGs regardless of depth in clean reads. Downstream analyses were performed based on CpGs with equal or more than 5x depth coverage. Bisulphite conversion rate shows the percentage of Cs that converted to uracil during the bisulphite conversion process.

of embryos and investigation of sperm DNA methylation profiles by RRBS.

As we previously reported, significantly lower percentages of DFI and HDS were observed in sperm cells from bulls of high NR56 compared to bulls of low NR56 (Narud et al., 2020). In the present study, sperm DFI and HDS correlated positively with protamine deficiency. This corroborates the results of a previous study in bovine (Fortes et al., 2014). The protamine structure in the sperm nucleus is strongly stabilized through the formation of disulfide bonds between cysteine residues of adjacent protamine molecules (Oliva, 2006). Recently, our group discovered that DNA fragmentation had a significant but weak positive correlation with free thiols and disulfide bonds of boar spermatozoa (Khezri et al., 2019). In the present study, however, no associations were found between sperm thiols/disulfide bonds and DNA integrity or field fertility (NR56).

Spermatozoa from HF bulls displayed an increased ability to fertilize oocytes in vitro and resulted in significantly higher cleavage rates and total blastocyst rates than LF bulls. However, by measuring the number of cleaved cells that developed further into blastocysts, no differences were detected between the fertility groups. Our results corroborate the findings of Al Naib et al. (2011), which observed that once fertilization occurred the following embryo development into blastocysts was not influenced by the bulls' fertility status. Furthermore, Ward et al. (2001) observed that bull's field fertility measured as non-return rate after 150 days correlated with cleavage rate, while B. R. Zhang et al. (1997) found a positive correlation between NR56 and both cleavage and blastocyst rate. In contrast, Kropp et al. (2017) found no difference in cleavage or blastocyst rates between sires of contrasting fertility. The discrepancy between studies may be explained by factors such as the reliability of fertility data, number of ejaculates used per bull, how the experiments are conducted in lab and the range in fertility among the bulls included (Larsson & Rodríguez-Martínez, 2000).

The correlation analysis between NR56, chromatin integrity traits, and in vitro embryo development showed that both DFI and HDS were negatively correlated to the cleavage rate, but not to the blastocyst rate. This corroborated our findings that HF bulls had higher cleavage rates, but that the subsequent development of cleaved embryos into blastocysts was unaffected by bulls' fertility group. This is in agreement with the findings of a previous study, where sperm DNA damage, caused by increased oxidative stress, was found to affect cleavage rate (Simões et al., 2013). However, others have reported that DNA fragmentation in bull sperm does not impair IVF but rather the further embryonic development when the

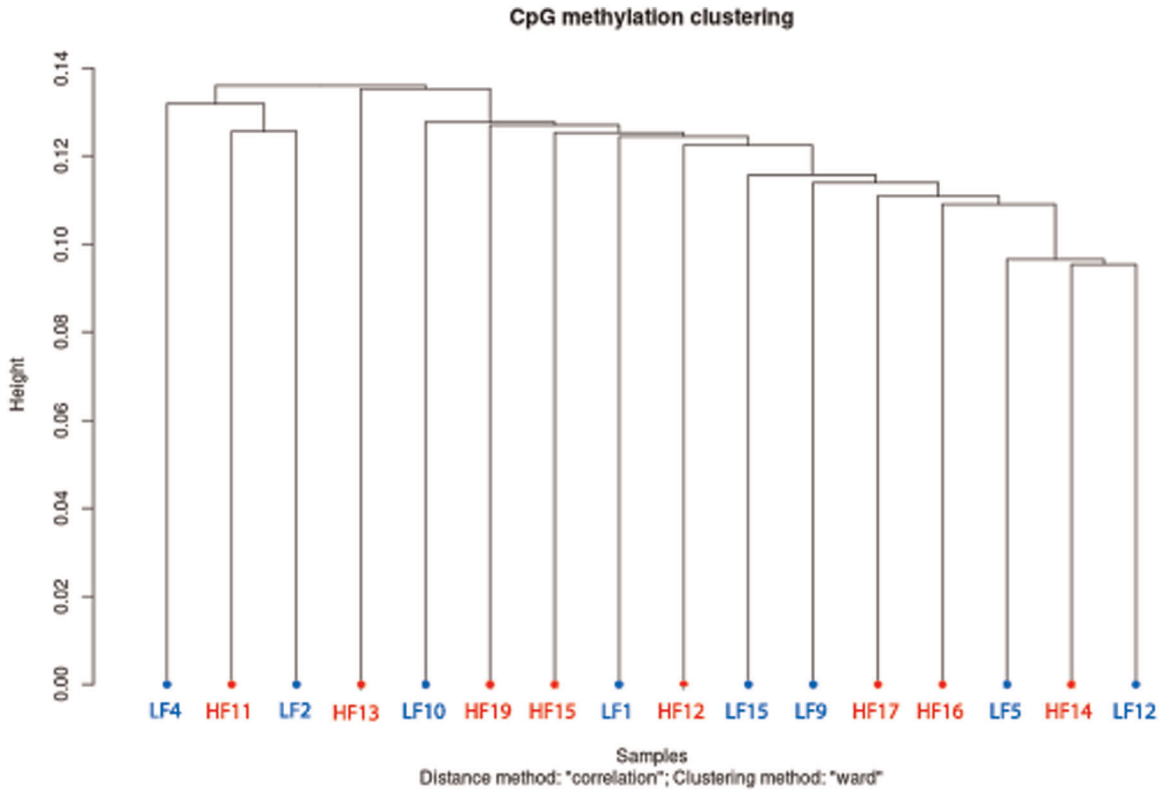

FIGURE 2 Hierarchical clustering of samples based on their CpG_{5x} methylation levels in sperm DNA (n = 16). Letters LF and HF suffixed by numbers indicates bulls with low and high NR56, respectively

blastocyst stage is reached (Fatehi et al., 2006). An important factor that may contribute to the observed results is the relatively low levels of DNA fragmentation in the Norwegian Red bulls of this study (ranging from 1.0% to 6.5%), which might be a result of selecting bulls with preferable semen quality for decades. It can be hypothesized that the level of fragmented DNA is within the range of damage that the oocytes manage to repair (García-Rodríguez et al., 2018). However, such repair is usually followed by early embryonic death, implantation defect, chromosomal abnormalities, and higher abortion rate (Tesarik et al., 2004), which might explain the strong negative association observed between DNA damage and NR56. This highlights the importance of elucidating sperm DNA integrity, especially when working with assisted reproductive technologies, such as IVF, where the natural selection of good quality sperm cells is excluded. It is important to mention that the number of developed blastocysts might have been insufficient to have enough power to detect a valid correlation between blastocyst rate and DFI and HDS. Thus, with a larger number of blastocysts it is possible that the correlation results

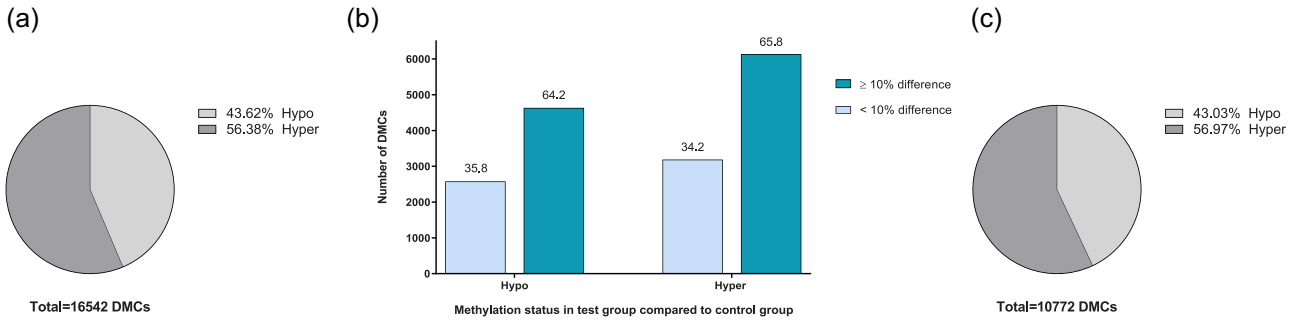

FIGURE 3 Numbers and degree of differentially methylated cytosines (DMCs) identified in the sperm DNA methylome between LF bulls (test) and HF bulls (control). (a) Total number of significant DMCs indicating that 56% are hypermethylated in the test group compared with the control group. (b) Levels of hypo- and hypermethylated cytosines in the test group compared to the control group. The numbers on the bars indicate the percentage in each respective bin. DMCs < 10% indicate cytosines with less than 10% difference in methylation level, while DMCs ≥ 10% indicate cytosines having equal and over 10% difference in methylation. (c) Number of filtered DMCs after applying a 10% methylation cut-off, which were used for downstream analyses

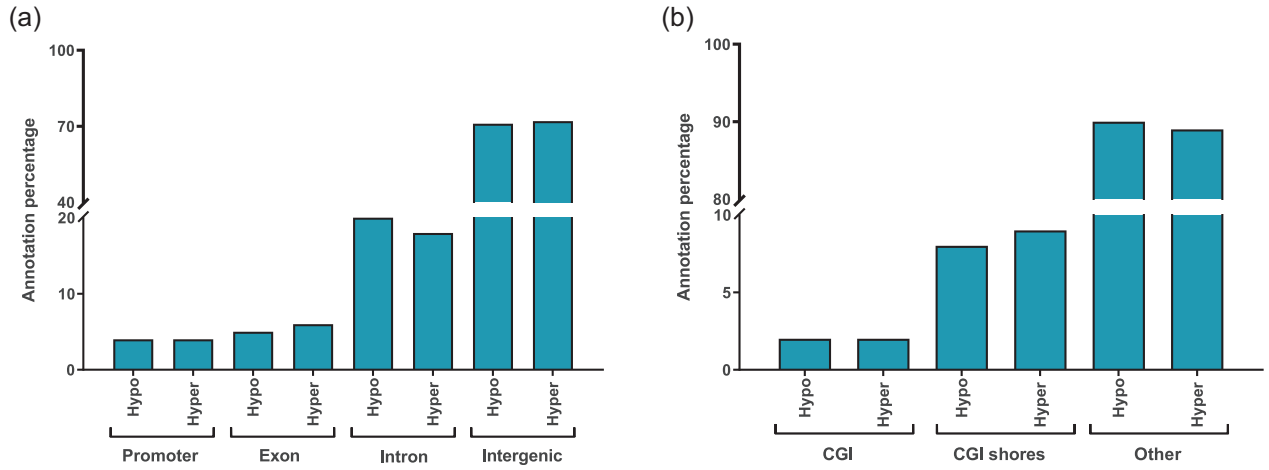

FIGURE 4 The distribution of filtered differentially methylated cytosines (DMCs) (methylation cut-off 10% and *q* value < 0.05) in the *bosTau9* genome. (a) Annotation of the hypo- and hypermethylated cytosines with gene features. (b) Annotation of the hypo- and hypermethylated cytosines with CpG features. CGI, CpG island; Hypo, hypomethylated cytosines; Hyper, hypermethylated cytosines

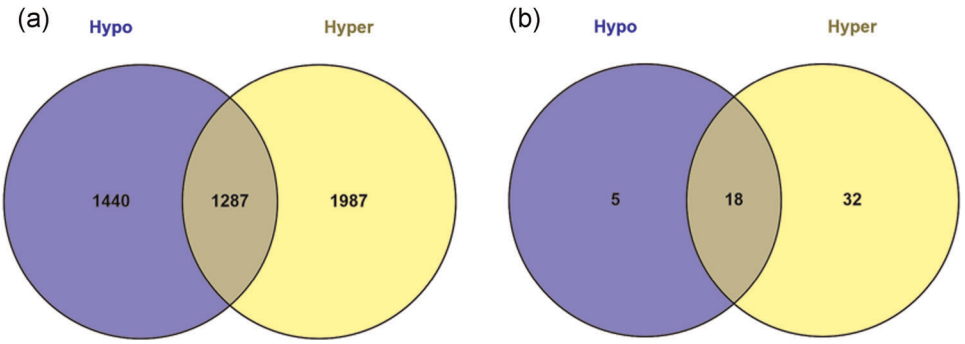

FIGURE 5 (a) Annotation of the filtered differentially methylated cytosines (DMCs) ≥ 10% to the nearest transcriptional start sites (TSSs). Numbers indicating the closest unique TSSs (duplicated TSSs removed) to DMCs ≥ 10% in hypomethylation (Hypo) and hypermethylation (Hyper) groups. (b) Number of significantly associated pathways to filtered DMCs ≥ 10% in hypomethylation (Hypo) and hypermethylation (Hyper) groups

TABLE 6 Number of genes representing different biological processes related to fertility, for which their transcriptional start sites were annotated with the Differentially methylated cytosines$_{\geq 10\%}$ in hypomethylated (Hypo) and hypermethylated (Hyper) groups

Fertility related biological process	Hypo	Hyper
Sperm motility	2	5
Sperm capacitation	1	2
Binding of sperm to zona pellucida	3	3
Acrosome reaction	1	3
Penetration of zona pellucida	0	2
Fertilization	9	13
Embryo implantation	6	9
In utero embryo development	30	33

would have been different. Furthermore, the total number of spermatozoa/mL added to the oocytes might have affected oocyte viability and cleavage. For some of the LF bulls, a higher total number of sperm was added due to lower sperm motility. Hence, harmful toxins and reactive oxygen species might have affected the cleavage rate where more dead spermatozoa were added. The higher degree of dead and dying oocytes for the LF bulls compared with HF bulls might also have affected the survival and development of those having been fertilized. However, our results showed that the variation in cleavage rate within the two fertility groups were close to similar.

The correlation analysis further indicated that there were no associations between sperm protamine deficiency and NR56 or with IVF outcomes. This is in agreement with a recent study by Castro et al. (2018), reporting that protamine deficiency in bovine spermatozoa might not have a strong biological impact in explaining difference of in vitro fertility between bulls due to the generally low

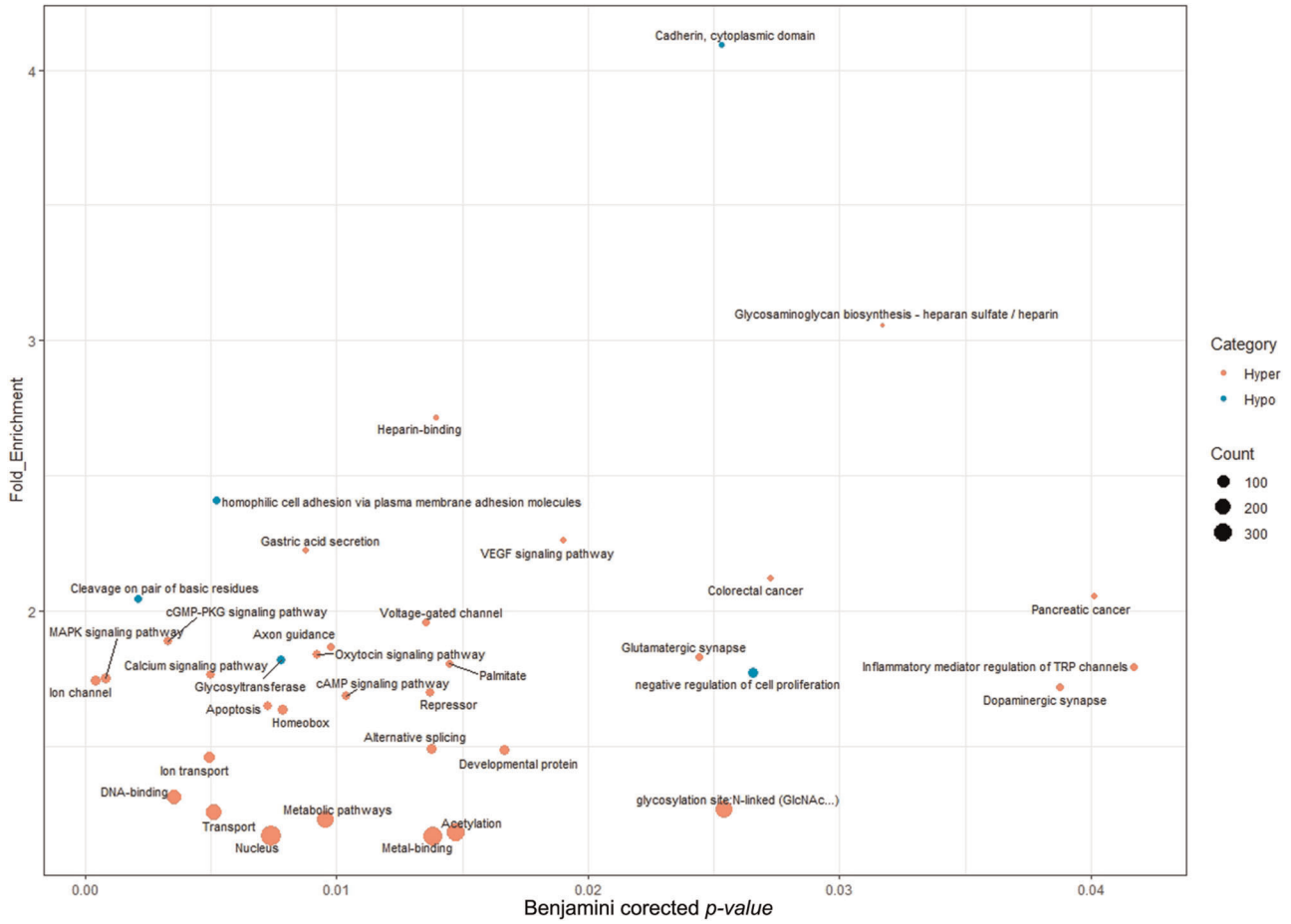

FIGURE 6 Exclusively identified pathways for annotated genes to differentially methylated cytosines (DMCs) ≥ 10%. Pathways are plotted in function of their Benjamini corrected *p* value (*x*-axis) and fold enrichment (*y*-axis). Gene count size key shows the number of genes involved in each pathway. Hypo, hypomethylated cytosines (referring to transcriptional start sites [TSSs] annotated with hypomethylated cytosines in test group); Hyper, hypermethylated cytosines (referring to TSSs annotated to hypermethylated cytosines in test group)

levels of protamine deficiency in bovine spermatozoa (Castro et al., 2018; Kipper et al., 2017).

In this study, the average global CpG methylation level was 42.8%. Recently, we reported similar results (global CpG methylation level of 40%) for bull sperm samples collected from young Norwegian Red bulls (Khezri et al., 2020). These results are in agreement with previous studies, where average global CpG methylation levels of 35% and 45% in bull sperm cells have been reported, using RRBS and a luminometric methylation assay, respectively (Jiang et al., 2018; Perrier et al., 2018). In the present study, the differential methylation analysis showed higher level of CpG methylation (hypermethylation) in samples from bulls of low NR56 compared to bulls of high NR56. Similar results have previously been reported for humans, where 74% of DMCs were hypermethylated in infertile patients (Camprubí et al., 2016). In addition, the present findings are supported by a study in buffalo, where a higher number of genes were hypermethylated in sub-fertile compared with high-fertile bulls (Verma et al., 2014). In contrast, Kropp et al. (2017) detected a higher level of methylated regions in sperm cells from high fertility Holstein bulls. This may be explained by the different techniques used for the study of sperm DNA methylation.

The regional analyses showed that on average 70% of the filtered DMCs were present in intergenic regions and over 85% of filtered DMCs were annotated within regions outside of CGI/CGI shores. These results are in agreement with previous studies on sperm DNA in bull (Jiang et al., 2018; Khezri et al., 2020; Perrier et al., 2018) and boar (Khezri et al., 2019). However, the results for intergenic regions are in contrast with data published in infertile human patients where only 33% of identified DMCs were annotated with intergenic regions (Camprubí et al., 2016).

In this study, functional analysis was used to identify some of the gene's biological processes related to fertility. The results indicated that a high number of genes represent biological processes such as in utero embryo development, fertilization, and embryo implantation, in both hypo- and hypermethylation groups, but with most genes represented in the hypermethylation group. For instance, genes such as transition protein 2 (*TNP2*) and T-box transcription factor T (*TBXT*), involved in penetration of zona pellucida, were exclusively identified in the hypermethylation group. Previous studies in mice have reported a relationship between premature translation of *TNP2* mRNA and the number of immobile and deformed sperm cells

(Tseden et al., 2007), and that deletion of the *TNP2* gene may result in less condensed sperm chromatin (Zhao et al., 2001). Data from Chinese Holstein bulls showed that the relative mRNA expression of *TNP1* gene was significantly associated with the degree of sperm cell deformities (S. Zhang et al., 2015). Currently, there are no data available on the role of *TBXT* gene in male fertility; therefore, this would be a fruitful area for further research.

One of the challenges in interpreting functional analysis results is that genes could be involved in several biological functions, simultaneously. Although several genes involved in fertilization were identified in this study, only three genes were identified with a single and specific biological process related to fertilization. These genes were zona pellucida binding protein (*ZPBP*) and regulated endocrine specific protein 18 (*RESP18*) in hypermethylated group and glioma pathogenesis-related 1-like protein 1 (*GLIPR1L1*) in hypomethylated group. Previous studies clearly demonstrated the significant role of *GLIPR1L1* in sperm-oocyte binding in mice and bovine (Caballero et al., 2012; Gaikwad et al., 2019; Gibbs et al., 2010). Furthermore, mice lacking *ZPBP* genes produced abnormal sperm cells with decreased ability to penetrate zona pellucida (Lin et al., 2007). In this study, the *RESP18* gene was connected to in utero embryo development. Previous studies reported that *RESP18* may have an important role in the development of nervous, cardiovascular, endocrine, renal, and reproduction systems (Atari et al., 2019). Furthermore, in agreement with our result, *RESP18* was previously identified as hypermethylated in low fertile buffalo bulls (Verma et al., 2014).

We have identified pathways related to fertilization and embryonic development that might explain the lower fertility performance of bulls with low NR56. For instance, oxytocin signaling, calcium signaling, ion channel/transport, voltage-gated channel, developmental proteins, and VEGF signaling pathways were discovered exclusively in the hypermethylation group of the test group (bulls with low NR56). In addition, we have recently shown that several intracellular sperm amino acids and trace elements are associated with field fertility and suggested that metabolomics may be a useful tool in the identification of biomarkers for male fertility (Narud et al., 2020). In accordance with this hypothesis, metal binding and metabolic pathways were found exclusively in the hypermethylation group, which might also explain the lower fertility in LF bulls. However, due to the high degree of transcriptome inactivity of sperm cells and unknown reproductive competence of females in this study, conclusion of involved pathways/genes in fertility output of LF bulls must be done with caution.

In conclusion, we show here that sperm DNA integrity is significantly associated with IVF capacity of Norwegian Red bulls. Spermatozoa of low-fertility bulls are hypermethylated compared with those of high-fertility bulls. Genes annotated to differentially methylated Cs were identified to participate in different biological pathways important for bull fertility.

ACKNOWLEDGMENTS

The authors wish to thank the Cells for Life platform at the Swedish University of Agricultural Sciences for the flow cytometry analyses of thiols, disulfide bonds, and protamine deficiency. Further, the authors would like to thank Geno Breeding and AI Association for providing samples and AI data for this study. Financial support was received from The Research Council of Norway (grant number 268048).

CONFLICT OF INTERESTS

The authors declare that there are no conflict of interests.

DATA AVAILABILITY STATEMENT

The data sets used and/or analyzed during the current study are available from the corresponding author on reasonable request.

REFERENCES

Akalin, A., Kormaksson, M., Li, S., Garrett-Bakelman, F. E., Figueroa, M. E., Melnick, A., & Mason, C. E. (2012). methylKit: A comprehensive R package for the analysis of genome-wide DNA methylation profiles. *Genome Biology*, *13*, R87. https://doi.org/10.1186/gb-2012-13-10-r87

Al Naib, A., Hanrahan, J. P., Lonergan, P., & Fair, S. (2011). In vitro assessment of sperm from bulls of high and low field fertility. *Theriogenology*, *76*, 161–167. https://doi.org/10.1016/j.theriogenology.2010.10.038

Alkhaled, Y., Laqqan, M., Tierling, S., Lo Porto, C., & Hammadeh, M. E. (2018). DNA methylation level of spermatozoa from subfertile and proven fertile and its relation to standard sperm parameters. *Andrologia*, *50*, e13011. https://doi.org/10.1111/and.13011

Atari, E., Perry, M. C., Jose, P. A., & Kumarasamy, S. (2019). Regulated endocrine-specific protein-18, an emerging endocrine protein in physiology: A literature review. *Endocrinology*, *160*, 2093–2100. https://doi.org/10.1210/en.2019-00397

Blondin, P., & Sirard, M. A. (1995). Oocyte and follicular morphology as determining characteristics for developmental competence in bovine oocytes. *Molecular Reproduction and Development*, *41*, 54–62. https://doi.org/10.1002/mrd.1080410109

Boe-Hansen, G. B., Fortes, M. R. S., & Satake, N. (2018). Morphological defects, sperm DNA integrity, and protamination of bovine spermatozoa. *Andrology*, *6*, 627–633. https://doi.org/10.1111/andr.12486

Boyle, P., Clement, K., Gu, H., Smith, Z. D., Ziller, M., Fostel, J. L., Holmes, L., Meldrim, J., Kelley, F., Gnirke, A., & Meissner, A. (2012). Gel-free multiplexed reduced representation bisulfite sequencing for large-scale DNA methylation profiling. *Genome Biology*, *13*, R92. https://doi.org/10.1186/gb-2012-13-10-r92

Caballero, J., Frenette, G., D'Amours, O., Belleannée, C., Lacroix-Pepin, N., Robert, C., & Sullivan, R. (2012). Bovine sperm raft membrane associated glioma pathogenesis-related 1-like protein 1 (GliPr1L1) is modified during the epididymal transit and is potentially involved in sperm binding to the zona pellucida. *Journal of Cellular Physiology*, *227*, 3876–3886. https://doi.org/10.1002/jcp.24099

Camprubí, C., Salas-Huetos, A., Aiese-Cigliano, R., Godo, A., Pons, M. C., Castellano, G., Grossmann, M., Sanseverino, W., Martin-Subero, J. I., Garrido, N., & Blanco, J. (2016). Spermatozoa from infertile patients exhibit differences of DNA methylation associated with spermatogenesis-related processes: An array-based analysis. *Reproductive BioMedicine Online*, *33*, 709–719. https://doi.org/10.1016/j.rbmo.2016.09.001

Castro, L. S., Siqueira, A. F. P., Hamilton, T. R. S., Mendes, C. M., Visintin, J. A., & Assumpção, M. E. O. A. (2018). Effect of bovine sperm chromatin integrity evaluated using three different methods on in vitro fertility. *Theriogenology*, *107*, 142–148. https://doi.org/10.1016/j.theriogenology.2017.11.006

Champroux, A., Cocquet, J., Henry-Berger, J., Drevet, J. R., & Kocer, A. (2018). A decade of exploring the mammalian sperm epigenome:

Paternal epigenetic and transgenerational inheritance. *Frontiers in Cell and Developmental Biology*, *6*, 50. https://doi.org/10.3389/fcell.2018.00050

Doherty, R., & Couldrey, C. (2014). Exploring genome wide bisulfite sequencing for DNA methylation analysis in livestock: A technical assessment. *Frontiers in Genetics*, *5*, 126–126. https://doi.org/10.3389/fgene.2014.00126

Fatehi, A. N., Bevers, M. M., Schoevers, E., Roelen, B. A. J., Colenbrander, B., & Gadella, B. M. (2006). DNA damage in bovine sperm does not block fertilization and early embryonic development but induces apoptosis after the first cleavages. *Journal of Andrology*, *27*, 176–188. https://doi.org/10.2164/jandrol.04152

Fortes, M. R., Satake, N., Corbet, D. H., Corbet, N. J., Burns, B. M., Moore, S. S., & Boe-Hansen, G. B. (2014). Sperm protamine deficiency correlates with sperm DNA damage in Bos indicus bulls. *Andrology*, *2*, 370–378. https://doi.org/10.1111/j.2047-2927.2014.00196.x

Gaikwad, A. S., Anderson, A. L., Merriner, D. J., O'Connor, A. E., Houston, B. J., Aitken, R. J., O'Bryan, M. K., & Nixon, B. (2019). GLIPR1L1 is an IZUMO-binding protein required for optimal fertilization in the mouse. *BMC Biology*, *17*, 86. https://doi.org/10.1186/s12915-019-0701-1

García-Rodríguez, A., Gosálvez, J., Agarwal, A., Roy, R., & Johnston, S. (2018). DNA Damage and repair in human reproductive cells. *International Journal of Molecular Sciences*, *20*, 31. https://doi.org/10.3390/ijms20010031

Gibbs, G. M., Lo, J. C. Y., Nixon, B., Jamsai, D., O'Connor, A. E., Rijal, S., Sanchez-Partida, L. G., Hearn, M. T. W., Bianco, D. M., & O'Bryan, M. K. (2010). Glioma pathogenesis-related 1-like 1 is testis enriched, dynamically modified, and redistributed during male germ cell maturation and has a potential role in sperm-oocyte binding. *Endocrinology*, *151*, 2331–2342. https://doi.org/10.1210/en.2009-1255

Gliozzi, T. M., Turri, F., Manes, S., Cassinelli, C., & Pizzi, F. (2017). The combination of kinetic and flow cytometric semen parameters as a tool to predict fertility in cryopreserved bull semen. *Animal*, *11*, 1975–1982. https://doi.org/10.1017/s1751731117000684

González-Marín, C., Gosálvez, J., & Roy, R. (2012). Types, causes, detection and repair of DNA fragmentation in animal and human sperm cells. *International Journal of Molecular Sciences*, *13*, 14026–14052. https://doi.org/10.3390/ijms131114026

Gu, H., Smith, Z. D., Bock, C., Boyle, P., Gnirke, A., & Meissner, A. (2011). Preparation of reduced representation bisulfite sequencing libraries for genome-scale DNA methylation profiling. *Nature Protocols*, *6*, 468–481. https://doi.org/10.1038/nprot.2010.190

Huang da, W., Sherman, B. T., & Lempicki, R. A. (2009). Systematic and integrative analysis of large gene lists using DAVID bioinformatics resources. *Nature Protocols*, *4*, 44–57. https://doi.org/10.1038/nprot.2008.211

Jiang, Z., Lin, J., Dong, H., Zheng, X., Marjani, S. L., Duan, J., Ouyang, Z., Chen, J., & Tian, X. (2018). DNA methylomes of bovine gametes and in vivo produced preimplantation embryos. *Biology of Reproduction*, *99*, 949–959. https://doi.org/10.1093/biolre/ioy138

Johnson, G. D., Lalancette, C., Linnemann, A. K., Leduc, F., Boissonneault, G., & Krawetz, S. A. (2011). The sperm nucleus: Chromatin, RNA, and the nuclear matrix. *Reproduction*, *141*, 21–36. https://doi.org/10.1530/rep-10-0322

Khezri, A., Narud, B., Stenseth, E. B., Johannisson, A., Myromslien, F. D., Gaustad, A. H., Wilson, R. C., Lyle, R., Morrell, J. M., Kommisrud, E., & Ahmad, R. (2019). DNA methylation patterns vary in boar sperm cells with different levels of DNA fragmentation. *BMC Genomics*, *20*, 897. https://doi.org/10.1186/s12864-019-6307-8

Khezri, A., Narud, B., Stenseth, E. B., Zeremichael, T. T., Myromslien, F. D., Wilson, R. C., Ahmad, R., & Kommisrud, E. (2020). Sperm DNA hypomethylation proximal to reproduction pathway genes in maturing elite Norwegian Red bulls. *Frontiers in Genetics*, *11*, 11. https://doi.org/10.3389/fgene.2020.00922

Kipper, B. H., Trevizan, J. T., Carreira, J. T., Carvalho, I. R., Mingoti, G. Z., Beletti, M. E., Perri, S. H. V., Franciscato, D. A., Pierucci, J. C., & Koivisto, M. B. (2017). Sperm morphometry and chromatin condensation in Nelore bulls of different ages and their effects on IVF. *Theriogenology*, *87*, 154–160. https://doi.org/10.1016/j.theriogenology.2016.08.017

Kropp, J., Carrillo, J. A., Namous, H., Daniels, A., Salih, S. M., Song, J., & Khatib, H. (2017). Male fertility status is associated with DNA methylation signatures in sperm and transcriptomic profiles of bovine preimplantation embryos. *BMC Genomics*, *18*, 280. https://doi.org/10.1186/s12864-017-3673-y

Krueger, F., & Andrews, S. R. (2011). Bismark: A flexible aligner and methylation caller for Bisulfite-Seq applications. *Bioinformatics*, *27*, 1571–1572. https://doi.org/10.1093/bioinformatics/btr167

Kumaresan, A., Das Gupta, M., Datta, T. K., & Morrell, J. M. (2020). Sperm DNA integrity and male fertility in farm animals: A review. *Frontiers in Veterinary Science*, *7*, 321–321. https://doi.org/10.3389/fvets.2020.00321

Larsson, B., & Rodríguez-Martínez, H. (2000). Can we use in vitro fertilization tests to predict semen fertility? *Animal Reproduction Science*, *60-61*, 327–336. https://doi.org/10.1016/S0378-4320(00)00089-0

Lin, Y. N., Roy, A., Yan, W., Burns, K. H., & Matzuk, M. M. (2007). Loss of zona pellucida binding proteins in the acrosomal matrix disrupts acrosome biogenesis and sperm morphogenesis. *Molecular and Cellular Biology*, *27*, 6794–6805. https://doi.org/10.1128/mcb.01029-07

Martin, M. (2011). Cutadapt removes adapter sequences from high-throughput sequencing reads. *EMBnet Journal*, *17*, 10–12. https://doi.org/10.14806/ej.17.1.200

Martínez-Pastor, F., Mata-Campuzano, M., Álvarez-Rodríguez, M., Álvarez, M., Anel, L., & De Paz, P. (2010). Probes and techniques for sperm evaluation by flow cytometry. *Reproduction in Domestic Animals*, *45*, 67–78. https://doi.org/10.1111/j.1439-0531.2010.01622.x

McSwiggin, H. M., & O'Doherty, A. M. (2018). Epigenetic reprogramming during spermatogenesis and male factor infertility. *Reproduction*, *156*, R9–r21. https://doi.org/10.1530/rep-18-0009

Meissner, A., Gnirke, A., Bell, G. W., Ramsahoye, B., Lander, E. S., & Jaenisch, R. (2005). Reduced representation bisulfite sequencing for comparative high-resolution DNA methylation analysis. *Nucleic Acids Research*, *33*, 5868–5877. https://doi.org/10.1093/nar/gki901

Ménézo, Y., Dale, B., & Cohen, M. (2010). DNA damage and repair in human oocytes and embryos: A review. *Zygote*, *18*, 357–365. https://doi.org/10.1017/s0967199410000286

Narud, B., Klinkenberg, G., Khezri, A., Zeremichael, T. T., Stenseth, E.-B., Nordborg, A., Haukaas, T. H., Morrell, J. M., Heringstad, B., Myromslien, F. D., & Kommisrud, E. (2020). Differences in sperm functionality and intracellular metabolites in Norwegian Red bulls of contrasting fertility. *Theriogenology*, *157*, 24–32. https://doi.org/10.1016/j.theriogenology.2020.07.005

Oliva, R. (2006). Protamines and male infertility. *Human Reproduction Update*, *12*, 417–435. https://doi.org/10.1093/humupd/dml009

Oliveros, J. C. (2015). *Venny. An interactive tool for comparing lists with Venn's diagrams.* https://bioinfogp.cnb.csic.es/tools/venny/index.html

Perrier, J. P., Sellem, E., Prézelin, A., Gasselin, M., Jouneau, L., Piumi, F., Al Adhami, H., Weber, M., Fritz, S., Boichard, D., Le Danvic, C., Schibler, L., Jammes, H., & Kiefer, H. (2018). A multi-scale analysis of bull sperm methylome revealed both species peculiarities and conserved tissue-specific features. *BMC Genomics*, *19*, 404. https://doi.org/10.1186/s12864-018-4764-0

Seligman, J., Kosower, N. S., Weissenberg, R., & Shalgi, R. (1994). Thiol-disulfide status of human sperm proteins. *Journal of Reproduction and Fertility*, *101*, 435–443. https://doi.org/10.1530/jrf.0.1010435

Simões, R., Feitosa, W. B., Siqueira, A. F. P., Nichi, M., Paula-Lopes, F. F., Marques, M. G., Peres, M. A., Barnabe, V. H., Visintin, J. A., & Assumpção, M. E. O. (2013). Influence of bovine sperm DNA fragmentation and oxidative stress on early embryo in vitro development outcome. *Reproduction*, *146*, 433–441. https://doi.org/10.1530/rep-13-0123

Standerholen, F. B., Myromslien, F. D., Kommisrud, E., Ropstad, E., & Waterhouse, K. E. (2014). Comparison of electronic volume and forward scatter principles of cell selection using flow cytometry for the evaluation of acrosome and plasma membrane integrity of bull spermatozoa. *Cytometry*, *85*, 719–728. https://doi.org/10.1002/cyto.a.22474

Tesarik, J., Greco, E., & Mendoza, C. (2004). Late, but not early, paternal effect on human embryo development is related to sperm DNA fragmentation. *Human Reproduction*, *19*, 611–615. https://doi.org/10.1093/humrep/deh127

Triantaphyllopoulos, K. A., Ikonomopoulos, I., & Bannister, A. J. (2016). Epigenetics and inheritance of phenotype variation in livestock. *Epigenetics & Chromatin*, *9*, 31. https://doi.org/10.1186/s13072-016-0081-5

Tseden, K., Topaloglu, Ö., Meinhardt, A., Dev, A., Adham, I., Müller, C., Wolf, S., Böhm, D., Schlüter, G., Engel, W., & Nayernia, K. (2007). Premature translation of transition protein 2 mRNA causes sperm abnormalities and male infertility. *Molecular Reproduction and Development*, *74*, 273–279. https://doi.org/10.1002/mrd.20570

UCSC. (2018). *Table browser for bosTau 9 assembly*. https://genome.ucsc.edu/cgi-bin/hgTables

Urrego, R., Rodriguez-Osorio, N., & Niemann, H. (2014). Epigenetic disorders and altered gene expression after use of assisted reproductive technologies in domestic cattle. *Epigenetics*, *9*, 803–815. https://doi.org/10.4161/epi.28711

Verma, A., Rajput, S., De, S., Kumar, R., Chakravarty, A. K., & Datta, T. K. (2014). Genome-wide profiling of sperm DNA methylation in relation to buffalo (Bubalus bubalis) bull fertility. *Theriogenology*, *82*(750–759), e751–759.e1. https://doi.org/10.1016/j.theriogenology.2014.06.012

Ward, F., Rizos, D., Corridan, D., Quinn, K., Boland, M., & Lonergan, P. (2001). Paternal influence on the time of first embryonic cleavage post insemination and the implications for subsequent bovine embryo development in vitro and fertility in vivo. *Molecular Reproduction and Development*, *60*, 47–55. https://doi.org/10.1002/mrd.1060

Waterhouse, K. E., Haugan, T., Kommisrud, E., Tverdal, A., Flatberg, G., Farstad, W., Evenson, D. P., & De Angelis, P. M. (2006). Sperm DNA damage is related to field fertility of semen from young Norwegian Red bulls. *Reproduction, Fertility, and Development*, *18*, 781–788. https://doi.org/10.1071/rd06029

Wickham, H. (2016). *ggplot2: Elegant Graphics for Data Analysis*. Springer-Verlag.

Zhang, B. R., Larsson, B., Lundeheim, N., & Rodriguez-Martinez, H. (1997). Relationship between embryo development in vitro and 56-day nonreturn rates of cows inseminated with frozen-thawed semen from dairy bulls. *Theriogenology*, *48*, 221–231. https://doi.org/10.1016/s0093-691x(97)84069-1

Zhang, S., Zhang, Y., Yang, C., Zhang, W., Ju, Z., Wang, X., Jiang, Q., Sun, Y., Huang, J., Zhong, J., & Wang, C. (2015). TNP1 functional SNPs in bta-miR-532 and bta-miR-204 target sites are associated with semen quality traits in Chinese holstein bulls. *Biology of Reproduction*, *92*, 139. https://doi.org/10.1095/biolreprod.114.126672

Zhang, X., Gabriel, M. S., & Zini, A. (2006). Sperm nuclear histone to protamine ratio in fertile and infertile men: Evidence of heterogeneous subpopulations of spermatozoa in the ejaculate. *Journal of Andrology*, *27*, 414–420. https://doi.org/10.2164/jandrol.05171

Zhao, M., Shirley, C. R., Yu, Y. E., Mohapatra, B., Zhang, Y., Unni, E., Deng, J. M., Arango, N. A., Terry, N. H. A., Weil, M. M., Russell, L. D., Behringer, R. R., & Meistrich, M. L. (2001). Targeted disruption of the transition protein 2 gene affects sperm chromatin structure and reduces fertility in mice. *Molecular and Cellular Biology*, *21*, 7243–7255. https://doi.org/10.1128/MCB.21.21.7243-7255.2001

Zhou, Y., Xu, L., Bickhart, D. M., Abdel Hay, E. H., Schroeder, S. G., Connor, E. E., Alexander, L. J., Sonstegard, T. S., Van Tassell, C. P., Chen, H., & Liu, G. E. (2016). Reduced representation bisulphite sequencing of ten bovine somatic tissues reveals DNA methylation patterns and their impacts on gene expression. *BMC Genomics*, *17*, 779. https://doi.org/10.1186/s12864-016-3116-1

Zubkova, E. V., Wade, M., & Robaire, B. (2005). Changes in spermatozoal chromatin packaging and susceptibility to oxidative challenge during aging. *Fertility and Sterility*, *84*(Suppl. 2), 1191–1198. https://doi.org/10.1016/j.fertnstert.2005.04.044

SUPPORTING INFORMATION

Additional Supporting Information may be found online in the supporting information tab for this article.

How to cite this article: Narud, B., Khezri, A., Zeremichael, T. T., Stenseth, E.-B., Heringstad, B., Johannisson, A., Morrell, J. M., Collas, P., Myromslien, F. D., & Kommisrud, E.. Sperm chromatin integrity and DNA methylation in Norwegian Red bulls of contrasting fertility. *Mol Reprod Dev*. 2021;88:187–200. https://doi.org/10.1002/mrd.23461